JOC*Article*

Crystallography and Magnetism of Two 1-(4-Nitroxylphenyl)pyrroles

Zeynep Delen and Paul M. Lahti*

Department of Chemistry, University of Massachusetts, Amherst, Massachusetts 01003

lahti@chem.umass.edu

Received August 4, 2006

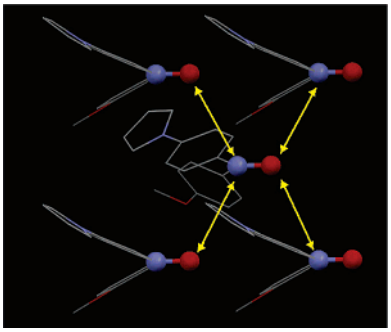

Stable radicals 1-(4-(*N*-*tert*-butyl-*N*-aminoxyl)phenyl)pyrrole (BNPP) and 1-(4-(*N*-[*para*-methoxyphenyl]-*N*-aminoxyl)phenyl)pyrrole (MNPP) were synthesized and characterized by crystallography and magnetism. BNPP crystals exhibit 1-D chains of intermolecular nitroxide NO to nitroxide CH_3 contacts, but polycrystalline magnetic susceptibility measurements show quite small antiferromagnetic (AFM) exchange interactions. MNPP shows stronger AFM exchange interactions that appear to be associated with a 2-D planar mesh of crystallographic nitroxide to nitroxide (N)O···N(O) contacts of 4.0−4.2 Å. The AFM behavior of MNPP can be fitted to a 2-D square planar Heisenberg antiferromagnetic exchange model with $J/k = (-)0.78 \pm 0.04$ K and mean field constant $\theta = (-)0.77 \pm 0.12$ K.

Introduction

Nitroxides have long been targets of substantial interest, due to their unusual stability among the family of organic radicals.[1] More recently, they have been much used as building blocks for molecular magnetic materials.[2] Conjugated nitroxides are particularly interesting, since they allow significantly more spin delocalization than nitronylnitroxides and iminoylnitroxides and thereby more chances for intermolecular exchange interactions in a crystal lattice between atoms bearing unpaired spin density. Most work has concentrated on aryl *tert*-butylnitroxides, which can delocalize onto one π-system. By comparison, diarylnitroxides can delocalize onto two aryl rings rather than one and are flatter molecules to allow possible closer packing. Although some diaryl nitroxides are stable enough to be studied spectroscopically, or even to use in spin labeling experiments,[3] few have been subjected to crystallographic and bulk magnetic analyses. DANO

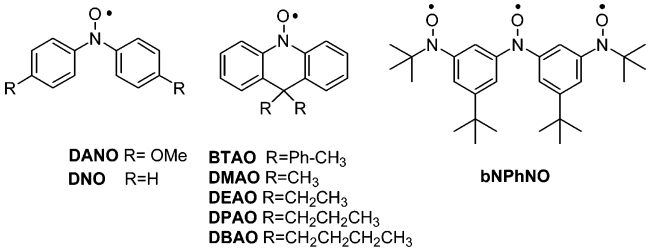

has been the most studied diarylnitroxide magnetic system.[4] Other examples are diphenyl nitric oxide (DNO),[5] its derivatives

(1) (a) Forrester, A. R.; Hay, J. M.; Thomson, R. H. *Organic Chemistry of Stable Free Radicals*; Academic Press: New York, 1968.

(2) (a) Rassat, A. *Pure Appl. Chem.* **1990**, *62*, 223. (b) Veciana, J.; Cirujeda, J.; Rovira, C.; Molins, E.; Novoa, J. J. *J. Phys. I.* **1996**, *6*, 1967. (c) Nakatsuji, S.; Anzai, H. *J. Mater. Chem.* **1997**, *7*, 2161. (d) Pilawa, B. *Ann. Phys.* **1999**, *8*, 191−254. (e) Itoh, K.; Kinoshita, M. *Molecular Magnetism: New Magnetic Materials*; Gordon and Breach: Newark, NJ, 2000. (f) Miller, J. S., Drillon, M., Eds. *Magnetism: Molecules to Materials*; Volumes I-V; Wiley-VCH: Weinheim. (g) Lahti, P.M. in *Carbon-based magnetism: An overview of the magnetism of metal-free carbon-based compounds and materials*; Palacio F., Markova, T., Eds.; Elsevier: Amsterdam, 2006; pp 23−52.

(3) (a) Calder, A.; Forrester, A. R. *J. Chem. Soc. C.* **1969**, 1459. (b) Forrester, A. R.; Hepburn, S. P.; McConnachie, G. *J. Chem. Soc. Perkin Trans.* **1974**, *1*, 2213. (c) Forrester, A. R.; Hepburn, S. P. *J. Chem. Soc. Perkin Trans. 1*, **1974**, 2208. (d) Keana, J. F. W. *Chem. Rev.* **1978**, *78*, 37.

10.1021/jo0616299 CCC: $33.50
Published on Web 11/04/2006

BTAO,[6] DMAO, DEAO, DBAO and DPAO,[7] and bis[3-*tert*-butyl-5-(*N*-*tert*-butylaminoxyl)phenyl]nitroxide (bNPhNO).[8]

The attachment of conjugating heteroarene substituents provides an important strategy for modulating spin density distributions, crystal packing, and magnetic exchange in solid nitroxide radicals.[9] This article describes the synthesis and magnetostructural characterization of two *para*-nitroxylphenylpyrroles, 1-(4-(*N*-*tert*-butyl-*N*-aminoxyl)phenyl)pyrrole (BPNPP) and 1-(4-(*N*-[*para*-methoxyphenyl]-*N*-aminoxyl)phenyl)-pyrrole (MNPP).

Results

Synthesis. BNPP and MNPP were synthesized as shown in Scheme 1. Initially, BNPP was pursued by palladium diacetate catalyzed C−N bond formation between pyrrole and BrPhNITBDMS to give BNPPTBDMS, followed by deprotection to BNPPH and oxidation to the radical (route 1). This route did afford milligram quantities of BNPP, but the initial coupling step gave lower yields than was desirable, given the effort of making[10] BrPhNITBDMS. Route 2 turned out to be better for us, via a high yield condensation of 4-bromobenzaldehyde with 2,5-dimethoxytetrahydrofuran to give pyrrole BrPP, followed by metalation, reaction with 2-methyl-2-nitrosopropane[11] to give BNPPH, and oxidation with PbO_2 to yield BNPP. Similarly, MNPP was made by metalation of BrPP and reaction with 4-nitrosoanisole;[12] the presumed MNPPH was not isolated but oxidized directly in air to give the radical. Both product radicals are deep red-purple, crystalline solids that show no evidence of decomposition after months of exposure to air at room temperature.

ESR Spectroscopy. Table 1 summarizes hyperfine coupling constants (hfc) derived from the X-band solution ESR spectroscopy at 200−300 K and includes comparisons to computational hfc estimates. Spin density populations computed[13] using the UB3LYP/6-31G* hybrid density functional[14] (at crystallographic molecular geometries described in the following section) were converted to predicted hfc using the McConnell relationship,[15] eq 1. Here, a_X is the predicted hfc from atom X, ρ is the spin density on nitrogen for a_N or on the attached π-carbon for an aryl hydrogen atom: values of $Q_N = 30$ G and $Q_H = (-)22$ G were used.

$$a_X = Q_X\rho \qquad (1)$$

SCHEME 1. Syntheses of BNPP and MNPP

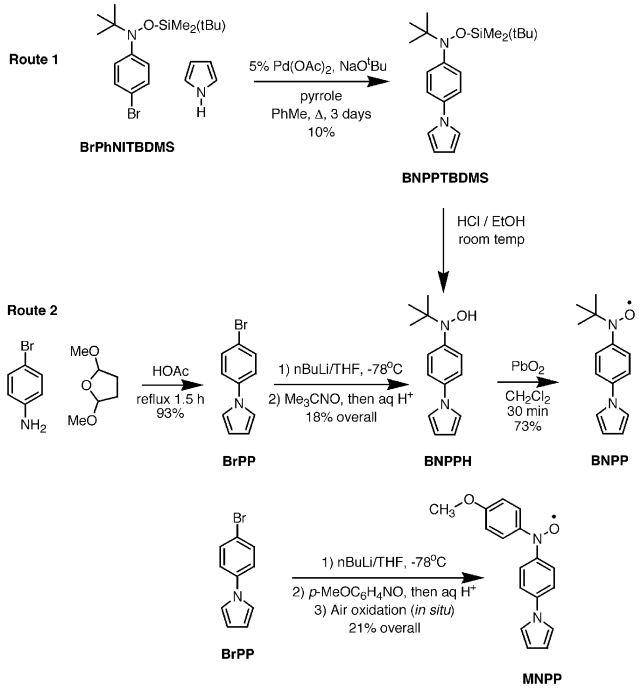

Crystallography. The radicals were studied by single-crystal X-ray diffraction at room temperature. Figure 1 shows ORTEP style diagrams[16] of the molecular structures. Further crystallographic details are summarized in the experimental section and in supporting material, including selected structural and intermolecular contact parameters.

Magnetic Measurements. Figures 2 and 3 show temperature versus paramagnetic susceptibility (χ) data for the radicals. The solid and dashed line functions in the figures come from analyses that are described in the discussion section below. Magnetization versus field measurements also were carried out for the samples at 1.8 K; details are given in the Experimental Section and in the Supporting Information.

Discussion

Molecular Spin Density Distributions. An important reason for choosing arylnitroxide building blocks for molecular magnetism is their ability to delocalize unpaired spin to some extent. The ESR spectra and computational spin density analyses show where the significant spin density populations are located in BNPP and MNPP. BNPP shows significant delocalization onto its phenyl ring. Hfc from the *tert*-butyl group on BNPP was not resolved: comparison to hyperfine deduced for di-*tert*-butylnitroxide and structurally related nitroxides suggests[17] that this would be ∼0.1 G or less. MNPP shows delocalization onto both aryl rings, somewhat more on the phenylene than the anisyl ring. Neither radical shows significant spin delocalization onto the pyrrole rings.

From Table 1, the largest delocalized spin populations lie on the protons *ortho* to the nitroxides (7−9%); the second largest lie on the *meta* protons (4−7%). The anisole proton hfc are smaller than those on the phenyl ring of MNPP, but still

(4) (a) Duffy, W. J.; Strandburg, D. L.; Deck, J. F. *Phys. Rev.* **1969**, *183*, 567. (b) Takizawa, O. *Bull. Chem. Soc. Jpn.* **1976**, *49*, 583.
(5) Takizawa, O.; Yamauchi, J.; Ohya-Nishiguchi, H.; Deguchi, Y. *Bull. Chem. Soc. Jpn.* **1971**, *44*, 3188.
(6) Imachi, R.; Ishida, T.; Suzuki, M.; Yasui, M.; Iwasaki, F.; Nogami, T. *Chem. Lett.* **1997**, *8*, 743.
(7) Nakagawa, M.; Ishida, T.; Suzuki, M.; Hashizume, D.; Yasui, M.; Iwasaki, F.; Nogami, T. *Chem. Phys. Lett.* **1999**, *302*, 125.
(8) Ishida, T.; Iwamura, H. *J. Am. Chem. Soc.* **1991**, *113*, 4238.
(9) Cf. a review in Lahti, P. M. "Magneto-structural Correlations in π-Conjugated Nitroxide-based Radicals: Hydrogen-bonds and Related Interactions in Molecular Organic Solids", in *Carbon-based magnetism: An overview of the magnetism of metal-free carbon-based compounds and materials*; Palacio, F., Markova, T., Eds.; Elsevier: Amsterdam, The Netherlands, 2006; pp 23−52.
(10) Field, L. M.; Lahti, P. M. *Chem. Mater.* **2003**, *15*, 2861.
(11) Stowell, J. C. *J. Org. Chem.* **1971**, *36*, 3055.
(12) Defoin, A. *Synthesis*, **2004**, *5*, 706.
(13) Computations were carried out using UNIX Spartan 2000 from Wavefunction, Irvine, CA.
(14) Becke, A. D. *J. Chem. Phys.* **1993**, *98*, 5648.
(15) McConnell, H. M. *J. Chem. Phys.* **1956**, *24*, 764.
(16) Farrugia, L. J. *J. Appl. Cryst.* **1997**, *30*, 565.
(17) (a) Faber, R. J.; Markeley, F. W.; Weil, J. A. *J. Chem. Phys.* **1967**, *46*, 1652. (b) Bales, B. L.; Peric, M.; Lamy-Freund, M. T. *J. Magn. Res.* **1998**, *132*, 279.

TABLE 1. Experimental and Computed hfc for BNPP and MNPP[a]

BNPP		MNPP	
experimental	estimated	experimental	estimated
11.74	11.8 (nitroxide N)	9.73	10.0 (nitroxide N)
		1.72	1.5 (anisole CH ortho to NO)
			0.8 (anisole CH meta to NO)
2.22	2.0 (CH ortho to NO)	1.98	2.0 (phenyl CH ortho to NO)
0.90	1.1 (CH meta to NO)	0.89	1.1 (phenyl CH meta to NO)
	0.04 (pyrrole 2,5 CH)		0.04 (pyrrole 2,5 CH)
	0.13 (pyrrole 3,4 CH)		0.15 (pyrrole 3,4 CH)
	−0.01 (pyrrole N)		<0.01 (pyrrole N)
	<0.0025 (*tert*-Bu C-H)		*<0.001* (methoxy CH)

[a] All hfc in gauss. Experimental hfc from ESR spectroscopy; non-italic estimated hfc from UB3LYP/6-31G* spin density computations with conversion using eq 1 ($Q_N = 30$ G, $Q_H = -22$ G); italic estimated hfc for sp^3 CH taken directly from computations.

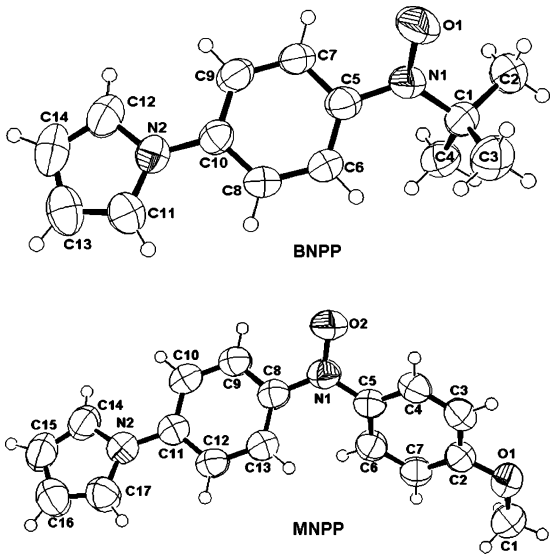

FIGURE 1. ORTEP diagrams for BNPP and MNPP. Thermal ellipsoids shown at 50% probability.

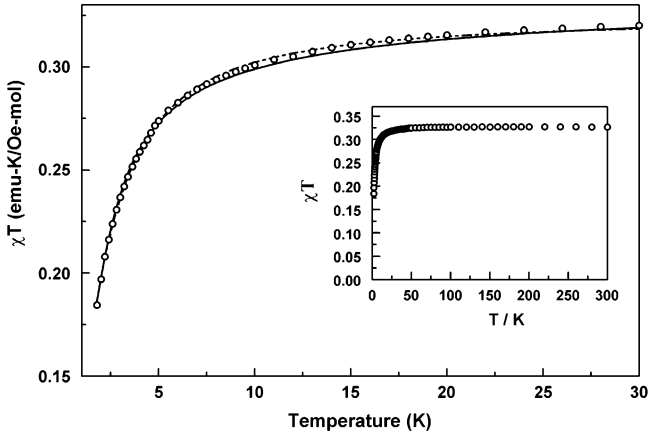

FIGURE 2. χT versus T plot for polycrystalline BNPP at 1000 Oe. Inset shows full temperature range of the experiment, 1.8−300 K. Broken line shows spin−pairing fit, and solid line shows 1-D AFM chain fit to data.

significant at the position *ortho* to the nitroxide. The phenyl rings therefore bear enough spin density to provide potential intermolecular exchange interactions at close enough contact distances. Since spin density in MNPP is spread onto two aryl rings, it has more possibilities for intermolecular solid-state exchange contacts.

The computed spin density patterns show that the radicals conform to typical expectations of spin polarization behavior, with alternating signs of spin density on the phenyl rings that are in direct resonance conjugation with the nitroxide groups. The nitroxides themselves are computed to retain over 80% of the total spin density, and the rest is mostly delocalized onto the phenyl rings, with quite small populations on other moieties. No more than 0.7% spin population is predicted on any CH of the pyrroles (Table 1), and ≤0.25% spin population is predicted on any BNPP *tert*-butyl group proton (depending on conformational placement in the latter). These results are in good accord with the experimental observations and provide a reasonable basis for attempting to understand intermolecular exchange in the crystal structures of the two radicals.

Crystallographic Close Contacts. BNPP crystallizes in the orthorhombic $Pna2_1$ space group. The closest intermolecular contacts between NO units are all >5.4 Å, sufficiently long to rule out significant direct interaction between these major spin density sites. The closest intermolecular contacts with the NO units are to the CH bonds on nearby *tert*-butyl, as shown in Figure 4, with r[(N)O···H(C,*tert*-butyl)] ∼ 2.6 Å. There are no close contacts between the nitroxides and any aryl CH bonds. Since there are no close intermolecular contacts between the groups bearing significant spin densities, any intermolecular exchange would result from through-space dipole−dipole interactions or spin−polarization interactions involving the very small spin densities on the *tert*-butyl or pyrrole groups. Aryl CH/π-cloud herringbone T-type contacts between phenyl and pyrrole rings help to hold BNPP molecules together in the lattice, but they do not provide additional close contacts between sites bearing significant spin density.

MNPP crystallizes in the monoclinic *Cc* space group. The vectors of all NO bonds point essentially along the crystallographic *b*-axis. Unlike BNPP, MNPP has both nitroxide to aryl CH (N)O···HC contacts at distances of 2.7−2.9 Å, and (N)O···N(O) contacts at moderate distances of about 4.1 Å. Both types of contacts are shown in Figure 5. $(CH_3)O\cdots H_3C(O)$ dipolar interactions as well as phenyl/phenyl and pyrrole/ pyrrole CH/π-cloud herringbone T-type contacts bring the MNPP molecules into close contact throughout the lattice, forming unusual 2-D sheets of nitroxide−nitroxide contacts shown in Figure 6. Pyrrole−anisole CH···$(O)CH_3$ dipolar contacts associate neighboring sheets at a plane to plane distance of 15 Å. The combination of these various relatively weak dipolar and induced dipolar interactions in MNPP causes it to crystallize to form sheet-like regions of high spin density sites (the nitroxides) that are widely separated by regions with very little spin density.

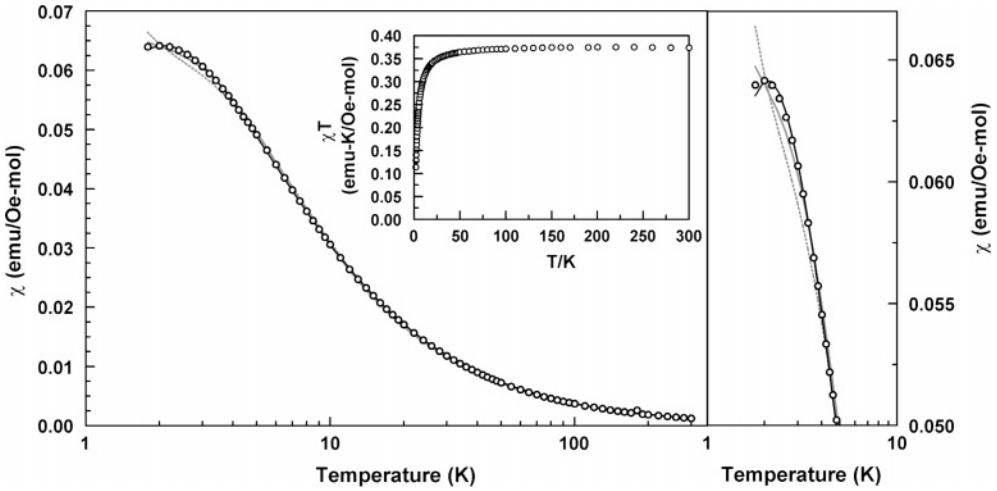

FIGURE 3. χ versus T plots for polycrystalline MNPP at 1000 Oe, 1.8−300 K (left) and 1.8−10 K (right). Inset shows full temperature range plot of the $\chi T(T)$ data, 1.8−300 K. Broken gray line shows spin−pairing fit, solid gray line shows 1-D AFM chain fit, and solid black line shows 2-D square planar AFM model fit to data.

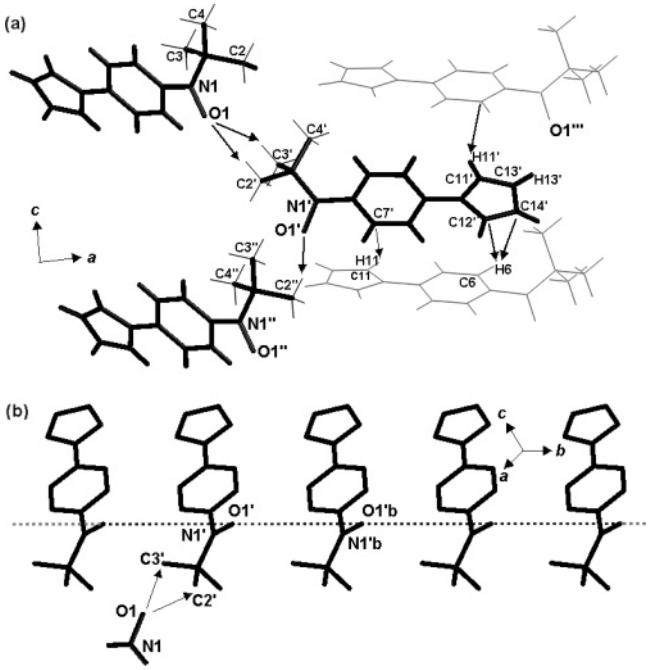

FIGURE 4. Close contacts in BNPP involving nitroxide groups. Part a shows nitroxide-HC contacts, and part b shows nitroxide−nitroxide contacts, with relation to nitroxide-HC contacts from part a. See also Supporting Information.

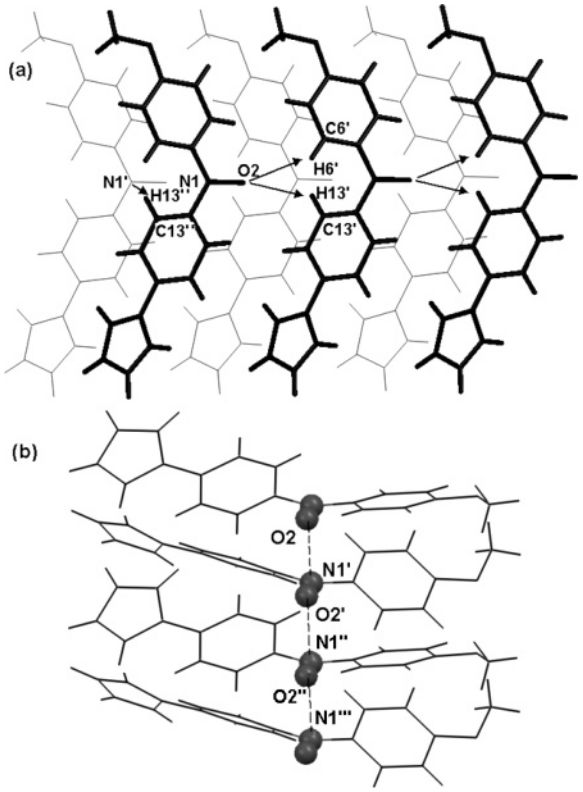

FIGURE 5. Close contacts in MNPP involving nitroxide groups. Part a shows nitroxide-HC contacts, and part b shows nitroxide−nitroxide contacts. See also Supporting Information.

Magnetostructural Analysis of BNPP: Curie−Weiss analysis ($1/\chi$ versus T, see Supporting Information) and the high-temperature limiting value of the $\chi T(T)$ plot (Figure 2) for multiple samples of BNPP yields a Curie constant of $C = 0.33$ emu·K/Oe·mol. Although this value is a bit small (possibly due to hygroscopic water uptake during sample preparation), it is quite consistent with $S = {}^1/_2$ spin carriers. The Weiss constant is virtually zero, showing near isolation of paramagnetic spins. The $\chi T(T)$ data decrease to about 0.18 emu·K/Oe·mol as the temperature decreases below ~30 K, showing weak antiferromagnetic (AFM) exchange interactions. Nonlinear least-squares fits were carried out using spin-pairing[18] and antiferromagnetic Heisenberg 1-D chain[19] expressions, with variation of the sample Landé constant, exchange constant, and a generalized mean field constant; g, J/k, and θ, respectively. The fitted curves are shown in Figure 2, and the model equations given in Supporting Information.

For the spin-pairing fit, $g = 1.861 \pm 0.008$, $J/k = (-)3.7 \pm 0.2$ K, and $\theta = (-)2.35 \pm 0.03$ K; for the 1-D chain fit, $g = 1.881 \pm 0.002$, $J/k = (-)1.3 \pm 0.2$ K, and $\theta = (-)0.5 \pm 0.2$

(18) Bleaney, B.; Bowers, K. D. *Proc. R. Soc. London A* **1952**, 214.

(19) (a) Bonner, J. C.; Fisher, M. E. *Phys. Rev. A* **1964**, *135*, 650. (b) Bonner, J. C.; Ph.D. Dissertation, University of London, U.K., 1968.

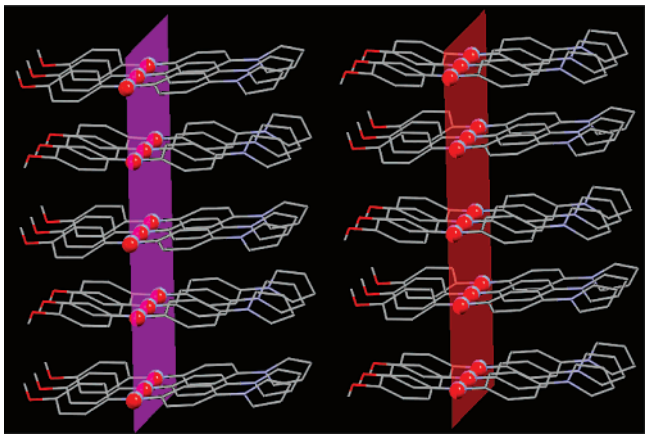

FIGURE 6. Planar sheets of spin density in MNPP, showing edge-on view of packing between two sheets. Red atoms are nitroxide oxygens; cyan atoms are nitrogens.

SCHEME 2. Close Contacts and Presumed Spin Polarization in BNPP

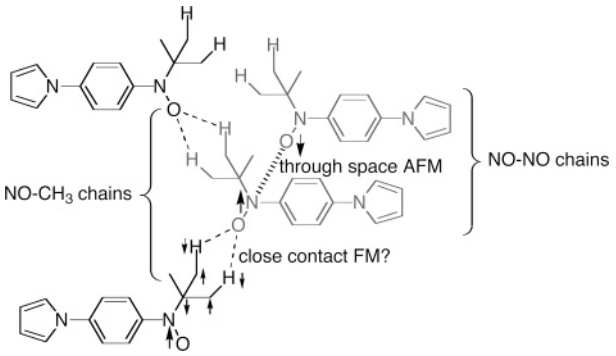

K; uncertainties are 95% confidence limits. Both fits deviate somewhat from the data in the 5−30 K region, and the large value of the Weiss constant for the spin-pairing fit suggests that this model is imprecise. Also, BNPP has no nitroxide dimeric contacts that are reasonably associated with spin-pairing exchange.

BNPP does have two chain contact motifs involving high spin density sites (Figure 4): (1) nitroxide/nitroxide contacts and (2) nitroxide···HC(*tert*-butyl) contacts. Scheme 2 shows a simplified representation of AFM exchange through chains of NO···NO contacts. These should be very weak due to the distances involved—5.7−5.8 Å for O(1)···O(1′b) and O(1′)···N(1′b)—in qualitative accord with the observed magnetic behavior. The closest contacts of the large nitroxide spin densities are with *tert*-butyl groups at (N)O···H(C) distances of 2.6−2.8 Å (based on O(1)···C′(2) and O(1)···C′(3) distances; see Supporting Information). The computed spin populations of the *tert*-butyl CH groups are very small (Table 1), with absolute sign depending on conformation relative to the NO group. Simplistic connectivity-only spin polarization considerations suggest FM exchange, as shown in the Scheme 2. However, the very small spin density populations on the nitroxide *tert*-butyl group make such chains at best a weak pathway for exchange. Since the experimental AFM exchange is so weak, a confident assignment to one of these mechanisms—or other, less well-defined through-space interaction such as dipole−dipole exchange—is not possible. Overall, BNPP is best described as having nearly paramagnetic behavior with only weak AFM interactions between molecules.

SCHEME 3. Close Contacts and Presumed Spin Polarization in MNPP

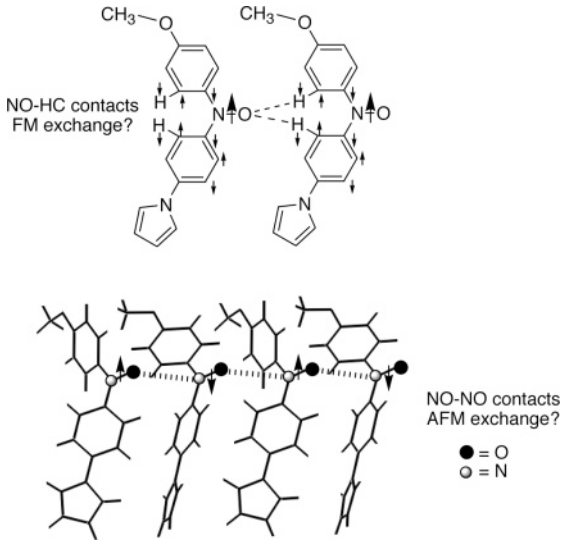

Magnetostructural analysis of MNPP. For χT(T > 100 K), MNPP has a Curie constant of 0.37 emu·K/Oe·mol, in excellent agreement with the value for $S = {}^1/_2$ spin carriers. The $\chi T(T)$ data below 100 K show significant deviation from isolated paramagnetic behavior, dropping to ∼0.12 emu·K/Oe·mol at 1.8 K. $\chi(T)$ also shows a maximum at about 2 K, near the minimum temperature accessible in these experiments; this indicates significantly stronger exchange interactions than observed in BNPP. The $\chi(T)$ plots are virtually identical at 300, 1000, and 10 000 Oe, showing no field-dependent saturation or metamagnetic effects.

The $\chi(T)$ data were fit using the same models as were used for BNPP; the results are shown in Figure 3. For the spin-pairing fit, $g = 2.065 \pm 0.086$, $J/k = (-)7.5 \pm 3.6$ K, and $\theta = (-)5.9 \pm 0.7$ K; for a 1-D chain fit, $g = 1.994 \pm 0.006$, $J/k = (-)2.09 \pm 0.05$ K, and $\theta = (-)0.41 \pm 0.04$ K. The fits were much poorer if mean-field terms θ were not included. The spin-pairing model deviates significantly from the data for $T < 4.5$ K, and the statistical uncertainties in its fitted parameters are large. This is consistent with a lack of crystallographic dimer contacts between nitroxide groups that could yield spin-pairing

The 1-D chain fit is better, although it shows some deviation from the data below about 3 K. As described in the crystallography section (Figure 5), there are two chain contact motifs in MNPP: nitroxide to phenyl NO···HC contacts, and nitroxide−nitroxide NO···NO contacts. Applying the alternant spin density signs found in the computational modeling, an NO···HC chain is predicted to produce FM exchange, while through space NO···NO contacts favor AFM exchange; this is summarized in Scheme 3. The latter mechanism is in accord with the experimental result. The through space interaction between large spin density nitroxides at the (N)O···N(O) distances of 4.0−4.2 Å apparently outweighs interaction between the nitroxide and the (much smaller) aryl H−C spin density, even though the latter is a much closer contact at 2.7−2.9 Å.[20] Since the nitroxide spin density sites in MNPP are significantly closer together than in BNPP, the greater AFM exchange constant in

(20) Cf. a similar case of close contact NO···NO interactions overcoming closer contact NO···HC interactions in Ferrer, J. R.; Lahti, P. M.; George, C.; Oliete, P.; Julier, M.; Palacio, F. *Chem. Mater.* **2001**, *13*, 2447.

SCHEME 4. Simplified Representation of the Proposed 2-D Exchange Lattice That Can Arise from the Crystallography of MNPP[a]

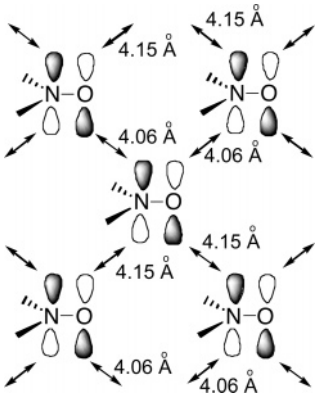

[a] Distances from Supporting Information.

MNPP makes sense if nitroxide−nitroxide contacts are the main mechanisms of exchange interaction.

Although the 1-D chain fit to the MNPP magnetic behavior is mathematically justifiable, crystallography suggests that the exchange interactions could propagate in a more complex manner. As shown in Figure 6, the MNPP NO···NO contacts form sheet-like planar meshes, with the planes strongly spin-isolated at distances of 15 Å. Scheme 4 shows one plane from Figure 6, with a top view of the unusual mesh of nearly equal N-to-O and O-to-N inter-nitroxide distances within the plane. The 2-π-center/3-electron electronic structure of the nitroxide units is not spatially isotropic in terms of spin density distribution, complicating the application of simplified magnetic lattice models. But, the crystallographic symmetry of the MNPP lattice places each nitroxide unit close to four other nitroxides in the planar mesh, with all interactions essentially occurring within the plane. This strongly suggests quasi 2-D square planar exchange between the spins. Effectively square planar magnetic behavior has been observed in other organic molecules having complex crystallographic close contact interactions. For example, 2-(*N*-*tert*-butyl-*N*-aminoxyl)benzimidazole (BABI) exhibits[21] quasi 2-D square planar type AFM magnetic exchange behavior, and thermodynamic measurements show it to behave[21c] as a 2-D Heisenberg square planar bilayer antiferromagnet with an ordering temperature of 1.7 K.

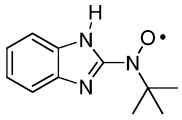

BABI

The magnetic data for MNPP were fit to a literature expression[22] for a Heisenberg 2-D AFM square planar system of $S = {}^1/_2$ spin units with a mean-field term; using the same variables as were described above, $g = 2.027 \pm 0.004$, $J/k = (-)0.78 \pm 0.04$ K, $\theta = (-)0.77 \pm 0.12$ K. The fit to the data is noticeably improved over the spin-pairing and 1-D chain fits (Figure 3). Caution is appropriate, since the maximum in the $\chi(T)$ plot is nearly at the low-temperature limit of our magnetometer—this may contribute to the fact that the exchange constant and the mean field constant are found to be nearly the same. Still, the network of crystallographic contacts between nitroxides (Scheme 4) and the good fit of a quasi 2-D square planar AFM exchange model to the susceptibility data both support describing MNPP exchange behavior in 2-D terms. Additional experiments will be required to find whether MNPP actual undergoes magnetic ordering as temperature decreases further.

Conclusions

BNPP and MNPP are both stable radicals, MNPP unusually so for a diarylnitroxide. BNPP is less spin delocalized than MNPP by ESR, based on both experimental hyperfine coupling data and computational studies; neither has significant spin density on the pyrrole rings. Because MNPP is more delocalized, it potentially can form more exchange-inducing contacts in a crystal lattice than BNPP. Although the pyrrole units do not bear spin density, they do contribute to the solid-state crystal lattice packing in both, primarily by participating in CH-π type contacts. Both radicals form noncentrosymmetric crystal lattices. The closest intermolecular contacts involving the nitroxide groups are NO···*tert*-Bu contacts in BNPP, NO···HC(aryl) contacts in MNPP. The antiferromagnetic behaviors of both systems are not consistent with a simple spin-polarization approach that emphasizes these closest contacts. Instead, exchange appears to be dominated by through space interactions between the nitroxide groups, quite weakly in BNPP at an inter-nitroxide distance of about 5.7 Å, more strongly in MNPP at about 4.0 Å. The variable temperature magnetism for BNPP fits a 1-D Heisenberg antiferromagnetic chain behavior with weak exchange. The magnetism and crystallographic packing of MNPP strongly suggests that its AFM exchange behavior is due to quasi 2-D square planar antiferromagnetic interactions. The unusual packing and magnetism of MNPP shows that an organic molecule that lacks strongly directional crystal assembly interactions (such as hydrogen bonds) can still form magnetically interesting crystal lattices.

Experimental

4-Nitrosoanisole. This compound was synthesized by a literature procedure to yield a green liquid at room temperature (lit. mp 22 °C[12]). ^{1}H NMR ($CDCl_3$): δ 3.95 (s, 3 H), 7.05 (d, 2 H, $J = 9.1$ Hz), 7.92 (broad d, 2 H).

1-(*para*-Bromophenyl)-*1H*-pyrrole (BrPP). This compound was made by a literature procedure. Mp: 86−90 °C, lit.[24] mp 86−90 °C. ^{1}H NMR ($CDCl_3$) δ 6.35 (t, 2 H, $J = 2.1$ Hz), 7.04 (t, 2 H, $J = 2.1$ Hz), 7.28 (*para* AA′BB′, 2 H, $J = 9.7$ Hz), 7.52 (*para* AA′BB′, 2 H, $J = 9.7$ Hz).

1-(4-(*N*-*tert*-butyl-*N*-hydroxylamino)phenyl)pyrrole (BNPPH). A solution of *n*-BuLi in hexanes (9.6 mL, 16.9 mmol) was slowly added to a solution of BrPP in 80 mL of anhydrous ether at −78 °C under nitrogen. The reaction was stirred for 1 h, during which it was allowed to warm to about −10 °C. A solution of 2-methyl-2-nitrosopropane[11] (1.5 g, 16.9 mmol) in 20 mL of anhydrous ether was then added dropwise to the reaction mixture. The mixture was allowed to stir under nitrogen overnight while

(21) (a) Ferrer, J. R.; Lahti, P. M.; George, C.; Antorrena, G.; Palacio, F. *Chem. Mater.* **1999**, *11*, 2205. (b) Lahti, P. M.; Ferrer, J. R.; George, C.; Oliete, P.; Julier, M.; Palacio, F. *Polyhedron* **2001**, *20*, 1465. (c) Miyazaki, Y.; Sakakibara, T.; Ferrer, J. R.; Lahti, P. M.; Antorrena, G.; Palacio, F.; Sorai, M. *J. Phys. Chem. B* **2002**, *106*, 8615.

(22) Baker, G., Jr.; Gilbert, H. E.; Eve, J.; Rushbrooke, G. S. *Phys. Lett.*, **1967**, *25A*(*3*), 207.

(23) Duling, D. R. *J. Magn. Res.* **1994**, *B104*, 105.

(24) Nakazaki, J.; Chung, I.; Matsushita, M. M.; Sugawara, T.; Watanabe, R.; Izuoka, A.; Kawada, Y. *J. Mat. Chem.* **2003**, *13*, 1011.

warming to room temperature, then quenched by careful, dropwise addition of excess saturated aqueous ammonium chloride The layers were separated, and the organic layer was washed with water. The combined aqueous layers were extracted with ether, and the combined organic layers were dried over anhydrous magnesium sulfate. The organic layers were evaporated, and the residue was subjected to column chromatography (silica, dichloromethane) to give the product as off yellow solid (0.59 g, 18%). This material was used as soon as possible in the next synthetic step. Mp: 145−147 °C. ^{1}H NMR ($CDCl_3$): δ 1.17 (s, 9 H), 5.11 (s, 1 H), 6.34 (t, 2 H, J = 2.6 Hz), 7.06 (t, 2 H, J = 2.6 Hz), 7.29 (s, 4 H). FT-IR (KBr, cm^{-1}): 3337−3016 (broad, O−H str), 2982−2900 (str, C−H str).

1-(4-(*N*-*tert*-butyl-*N*-aminoxyl)phenyl)pyrrole (BNPP). PbO_2 (1.13 g, 47 mmol) was added to a solution of BNPPH (0.27 g, 12 mmol) in dichloromethane. The reaction was monitored by TLC and found to be complete after half an hour. The reaction was filtered and evaporated, and the residue purified by column chromatography (silica, dichloromethane) to yield the radical as a red solid (0.20 g, 73%). Mp: 94−96 °C. Anal. calcd for $C_{14}H_{17}N_2O$: C, 73.33; H, 7.47; N, 12.22. Found: C, 73.07; H, 7.32; N, 12.10. ESR (9.592 GHz, toluene, 230 K): g = 2.00678, a_N = 11.74 G, a_{H1} = 2.22 G (2 H), a_{H2} = 0.90 G (2 H).

Crystallography: red needle from dichloromethane, using λ(Mo Kα) = 0.7107 Å, μ = 0.077 mm^{-1}, formula = $C_{14}H_{17}N_2O$, MW = 229.3, orthorhombic, space group $Pna2_1$, T = 298 K, Z = 4, a = 27.3232(12), b = 5.8054(2), c = 7.9936(4) Å, V = 1267.96(8) Å,^{3} D_{calc} = 1.201 g/cm^3, $F(000)$ = 492. A total of 2213 reflections were recorded at a threshold intensity of 2σ(I). A total of 2060 independent reflections were analyzed with 156 parameters using SHELXL-97.[25] The structure was checked for missing symmetry using the ADDSYM function of PLATON.[26] For 1642 reflections with $I > 2\sigma(I)$, $R_1(I > 2\sigma)$ = 0.0422, $wR_2(I > 2\sigma)$ = 0.1022; R_1(all) = 0.0613, wR_2(all) = 0.1140, goodness of fit on F^2 = 1.063. An absolute structure parameter of 0(2) was used. CCDC deposition no. 606967.

1-(4-(*N*-[*para*-Methoxyphenyl]-*N*-hydroxylaminoxyl)phenyl)-pyrrole (MNPP). A solution of *n*-BuLi in hexanes (2.6 mL, 5.6 mmol) was added to a solution of BrPP (1.0 g, 4.5mmol) in 10 mL of anhydrous ether at −78 °C under nitrogen. The reaction was stirred for 1 h, during which it was allowed to warm to about −10 °C. A solution of 4-nitrosoanisole[12] (0.8 g, 5.63 mmol) in 7 mL of anhydrous ether was then added to the reaction. The mixture was allowed to stir under nitrogen overnight while warming to room temperature, then quenched by careful, dropwise addition of excess saturated aqueous ammonium chloride. The layers were separated and the organic layer was washed with water, then the combined aqueous layers were extracted with ether. The combined organic layers were dried over anhydrous magnesium sulfate. Column chromatography (silica, dichloromethane) yielded the product as a red solid (0.26 g, 21% yield), which was recrystallized from dichloromethane. Mp: 184−185 °C Anal. calcd for $C_{17}H_{15}N_2O_2$: C, 73.10; H, 5.41; N, 10.03. Found: C, 72.40; H, 5.41; N, 9.94. ESR (9.6335 GHz, toluene): g = 2.00666, a_N = 9.73 G, a_{H1} = 1.98 G (2 H), a_{H2} = 1.72 G (2 H), a_{H3} = 0.89 G (2 H).

Crystallography: red needle from dichloromethane, using λ(Mo Kα) = 0.7107 Å, μ = 0.090 mm^{-1}, formula = $C_{17}H_{15}N_2O_2$, MW = 279.3, monoclinic, space group Cc, T = 293 K, Z = 4, a = 30.002(2) Å, b = 7.3588(4) Å, c = 6.2049(4) Å, β = 90.467(2)°, V = 1369.88(14) Å,^{3} D_{calc} = 1.354 g/cm^3, F(000) = 558. A total of 1314 reflections were recorded at a threshold intensity of 2σ(I). A total of 1217 independent reflections were analyzed with 192 parameters using SHELXL-97.[25] The structure was checked for missing symmetry using the ADDSYM function of PLATON.[26] For 1016 reflections with $I > 2\sigma(I)$, $R_1(I > 2\sigma)$ = 0.0608, $wR_2(I > 2\sigma)$ = 0.1029; R_1(all) = 0.0766, wR_2(all) = 0.1089, goodness of fit on F^2 = 1.279. CCDC deposition no. 606968.

Acknowledgment. This material is based upon work supported by the National Science Foundation under Grant CHE-0415716. We thank Dr. Peter Khalifah and Dr. Gregory Dabkowski for assistance with X-ray crystallography and microanalysis, respectively.

Supporting Information Available: Experimental procedures not included in the main text; HPLC traces, ESR spectra, and computational spin density summaries for BNPP and MNPP; magnetization versus field and Curie−Weiss data for BNPP and MNPP; magnetic models and hamiltonians used to fit variable temperature magnetic susceptibility data; a figure of nitroxide−nitroxide contacts in MNPP crystals; CIF crystallographic summary files for BNPP and MNPP. This material is available free of charge via the Internet at http://pubs.acs.org.

JO0616299

(25) Sheldrick, G. M. SHELXTL97 Program for the Refinement of Crystal Structures, University of Göttingen, Germany, 1997.

(26) (a) Le Page, Y. *J. Appl. Crystallogr.* **1987**, *20*, 264. (b) Le Page, Y. J. *J. Appl. Crystallogr.* **1988**, *21*, 983. (c) Spek, A. L. *J. Appl. Crystallogr.* **1988**, *21*, 578. (d) Spek, A. L. *Acta Crystallogr.* **1990**, *A46*, C34.